Uptake and Fate of Fluorescently Labeled DNA Nanostructures in Cellular Environments: A Cautionary Tale

4 authors, including:

Aurélie Lacroix
McGill University
5 PUBLICATIONS **36** CITATIONS

Empar Vengut-Climent
University of Valencia
18 PUBLICATIONS **56** CITATIONS

Hanadi F Sleiman
McGill University
165 PUBLICATIONS **5,082** CITATIONS

Some of the authors of this publication are also working on these related projects:

Cellular delivery with DNA nanostructures View project

Metal-DNA Nanostructures View project

Uptake and Fate of Fluorescently Labeled DNA Nanostructures in Cellular Environments: A Cautionary Tale

Aurélie Lacroix, Empar Vengut-Climent, Donatien de Rochambeau, and Hanadi F. Sleiman*

Department of Chemistry, McGill University, 801 Sherbrooke Street West, Montréal, Québec H3A 0B8, Canada

Ⓢ *Supporting Information*

ABSTRACT: Fluorescent dye labeling of DNA oligonucleotides and nanostructures is one of the most used techniques to track their fate and cellular localization inside cells. Here, we report that intracellular fluorescence, and even FRET signals, cannot be correlated with the cellular uptake of intact DNA structures. Live cell imaging revealed high colocalization of cyanine-labeled DNA oligos and nanostructures with phosphorylated small-molecule cyanine dyes, one of the degradation products from these DNA compounds. Nuclease degradation of the strands outside and inside the cell results in a misleading intracellular fluorescent signal. The signal is saturated by the fluorescence of the degradation product (phosphorylated dye). To test our hypothesis, we synthesized a range of DNA structures, including Cy3- and Cy5-labeled DNA cubes and DNA tetrahedra, and oligonucleotides with different stabilities toward nucleases. All give fluorescence signals within the mitochondria after cellular uptake and strongly colocalize with a free phosphorylated dye control. Kinetics experiments revealed that uptake of stable DNA structures is delayed. We also studied several parameters influencing fluorescent data: stability of the DNA strand, fixation methods that can wash away the signal, position of the dye on the DNA strand, and design of FRET experiments. DNA nanostructures hold tremendous potential for biomedical applications and biotechnology because of their biocompatibility, programmability, and easy synthesis. However, few examples of successful DNA machines *in vivo* have been reported. We believe this contribution can be used as a guide to design better cellular uptake experiments when using fluorescent dyes, in order to further propel the biological development, and application of DNA nanostructures.
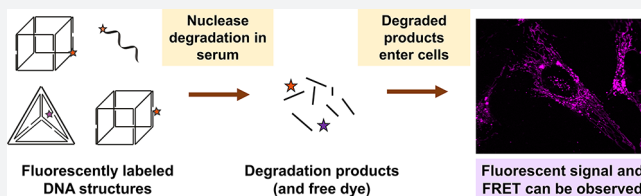
1. INTRODUCTION

DNA- and RNA-based therapeutics, such as antisense oligonucleotides, aptamers, small interfering RNAs, microRNAs, and the recently developed CRISPR-Cas9 editing tool, have emerged as highly promising strategies for disease treatment. Compared to small molecules, oligonucleotides are highly charged, have a high molecular weight, and are easily degradable by enzymes. Therefore, one essential element to their clinical success is their efficient intracellular delivery.[1] Poor stability and cellular permeability have hampered the development of these technologies.[2] The fate of these molecules has been extensively studied, yet they remain extremely complex to elucidate: many different possible cellular uptake pathways have been discovered. Differences observed arise from the sequence, the length of the oligonucleotide, or the use of chemical modifications, making almost every molecule unique in its uptake profile.[3]

More recently, the assembly of DNA and RNA into nanostructures has been explored as a method to deliver oligonucleotides and therapeutics.[2,4] DNA nanostructures are easily synthesized and highly programmable, such that arbitrary shapes and sizes can be efficiently designed.[5] Many examples in the literature have looked at their use in bioimaging, biosensing, or drug delivery.[6] These biocompatible constructs are more resistant to nuclease degradation than their single-stranded components and offer complete control over the

position of ligands.[7] They can be used to position drug-encapsulating polymers or protein-binding ligands.[8,9] They are also promising delivery tools for silencing oligonucleotides. For example, we showed that antisense strands positioned on DNA cages can induce higher gene silencing than the strands themselves, when transfected with lipofectamine.[10] DNA nanostructures can also be designed to be dynamic and signal responsive: they can release a therapeutic upon the recognition of a mRNA sequence, upon a change of pH, or with light.[11−13] All these results have demonstrated the potential to use DNA nanostructures as drug delivery systems. However, these structures face challenges similar to those faced by simple oligonucleotides because they are highly charged and degradable. One essential element that differs from linear oligonucleotides is their 3D shape, which has been proposed to trigger new uptake profiles.[6,14] Here again, structures will act differently according to sequence, length, and presence of chemical modification, but also its 3D shape and DNA density, making the analysis of each of these structures unique.

In 2011, Tuberfield et al. reported the cellular uptake of a double-stranded DNA tetrahedron in mammalian cells.[15] The study showed that cyanine 5 dye (Cy5)-labeled structures were taken up via endocytosis. By labeling the structure with biotin,

the authors measured that 2% of the initial tetrahedra was found inside the cell. Following this important publication, many groups have explored the uptake of DNA structures in cells.[14,16−18] However, we found that the literature on cellular uptake of DNA cages was somewhat ambiguous, uptake was not always quantified, and results greatly vary from one laboratory to another, due to differences in experimental design.[19] For example, for one structure (tetrahedron), studies report *minimal* cell uptake without transfection while other studies revealed *high* cell internalization.[20,21] In some cases, uptake was increased by the positioning of aptamers on the structure.[20,21] Other groups described no uptake of cyanine 3 dye (Cy3)-labeled DNA duplex but observed uptake of the tetrahedron inside cells, which is not consistent with the above-described first study, where single- and double-stranded controls were found inside the cell.[22] The sequence and length of the oligonucleotide used as a control is an important parameter that needs to be carefully studied. The uptake of larger structures, such as DNA origami, also remains elusive, and recent studies reported that it depends on both the nanoparticle shape and the cell line used.[23,24] Bastings et al. used oligolysine-based coating (to prevent degradation) on DNA structures to study their uptake,[24] while other groups studied the uptake of naked DNA origami.

On the other hand, it is important to highlight some of the successes made with DNA architectures. In particular, in 2012, a tetrahedron was decorated with folate to successfully deliver siRNAs *in vivo*.[25] A DNA icosahedron was used to encapsulate a fluorescent polymer to track pH changes in *Caenorhabditis elegans*.[26] DNA origami structures were also used as successful therapeutic robots by Church et al.[27] More recently, a DNA origami was functionalized with aptamers to target cancerous endothelial cells, and inhibition of tumor growth was demonstrated in mice and miniature pigs.[28] These examples demonstrate how careful design of either wireframe DNA architectures or DNA origami with chosen ligands can lead to a successful therapeutic device.

Overall, despite the explosion in the number of designs of DNA nanostructures, and some successes *in vivo*, the uptake of naked DNA architectures in cells remains ambiguous.[19] We believe there is a need to understand more precisely what governs the successful uptake of a 3D DNA structure and its intracellular fate in cells and in biological fluids. This will give greater insight into how to design better devices to achieve the desired therapeutic outcomes. In this paper, we highlight some important considerations that need to be taken into account when examining the uptake of DNA structures.

Under non-transfected conditions, uptake of naked DNA nanostructures is, in general, too low to observe any gene silencing, similar to oligonucleotides. Therefore, many groups have looked at uptake pathways by positioning a fluorescent dye on the structure and tracking the intracellular signal. Cyanine dyes, and fluorescein to a lesser extent, have been mostly used since they are available as phosphoramidites and therefore easy to attach to nucleic acids. However, the fluorophores themselves can cross the cellular membrane and accumulate in cell organelles.[29−31] We initially questioned whether the intracellular fluorescent signal corresponds to (i) dye-guided uptake of the structure (the dye interacts with the cellular membrane), (ii) degradation of the structure followed by uptake of the dye, or (iii) unaided cellular uptake of the intact DNA structure (the small-molecule dye does not play an important role). Our experiments revealed that the intracellular

fluorescence signal was caused by degradation of the DNA by extracellular nucleases, leading to release and uptake of the cyanine dyes. Phosphorylated dyes as models of degradation products were synthesized, incubated with cells, and colocalized perfectly with the signal from DNA structures. We showed that stabilizing the structure toward nuclease degradation simply delayed the intracellular fluorescent signal. Serum-free conditions, where extracellular nucleases are removed, or chemical fixation caused the disappearance of the signal. Finally, we showed that Förster resonance energy transfer (FRET), often used to assess integrity of a DNA structure inside the cells, needs more careful controls when performed. Notably, we could observe FRET between two separate, free phosphorylated dyes (Cy3 and Cy5) when they were co-incubated with cells.

2. DISCUSSION

Assembly of Structure and Design. In this study, we will focus on wireframe DNA architectures. Our group has developed DNA minimal nanocages such as cubes, prisms, and nanotubes. In particular, the DNA nanocube is composed of four DNA strands (96-mers component strands called "clips") that can self-assemble in a one-pot reaction with quantitative yields.[9] The DNA cube displays eight single-stranded regions (four on the top, and four on the bottom). A DNA tetrahedron was also prepared, as it is one of the most used structures in the literature.[17] The tetrahedron is also composed of four DNA strands but is fully double-stranded. We labeled both structures at the 5′-end with a cyanine dye using phosphoramidite chemistry: the tetrahedron was labeled with Cy5, and two clips were prepared for the cube, one with Cy3 and one with Cy5 (Figure 1). This labeling procedure has been commonly used in the literature.[6] Thermal assemblies were performed following previous protocols and assessed using gel electrophoresis (Figure S1).

Cellular Uptake of Cyanine-Labeled Oligonucleotide and DNA Nanostructures (5′-End). First, we compared the cellular uptake of the assembled nanostructure with the corresponding component strand (clip strand, 96-mer for the cube, 63-mer for the tetrahedron). If DNA nanostructures were taken up to a higher extent than their single-stranded components, via new internalization pathways due to their 3D
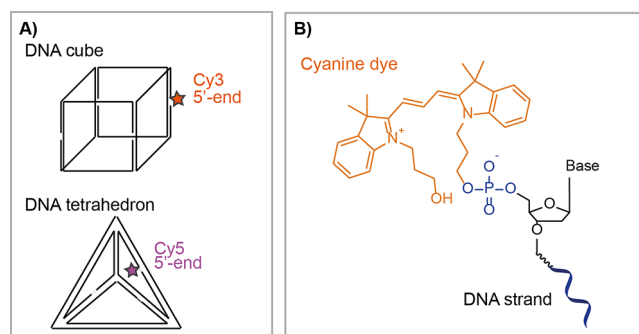

Figure 1. Cyanine-labeled DNA nanostructures. (A)Two wireframe DNA-minimal nanostructures were used in the study: the DNA nanocube, composed of four 96-mers, and the DNA tetrahedron, composed of four 63-mers. (B) Cyanine dyes (Cy3 on the schema) were attached at the 5′-end of one of the DNA component clips, using phosphoramidite chemistry and resulting in a phosphate linkage between the dye and the base.

shape, we would observe a difference in their uptake profile. Structures were added to FBS-containing media and tracked using confocal live microscopy in HeLa cells at different time points (1.5, 4, 6, and 24 h). After 1.5 h, we did not detect any signal for the structures, and the signal for the clips was very low, suggesting that uptake requires a longer time (Figure S9). At later time points (4, 6, and 24 h), we observed a similar uptake profile of the clip strands and the respective DNA nanostructures, consisting of very bright dots but also long filaments inside the cytoplasm of the cell (Figure 2 and Figures S2−S4 and S6−S8). The signals of the clip and the structure colocalize well (Figure S5).

To ensure that the cellular uptake of the component clip is not caused by their folding into secondary structures, which may mimic a 3D scaffold, we looked at the uptake of shorter 5′-end labeled DNA strands (20-mers) and a dinucleotide (Cy3-TG) (Figures S10 and S11). These short strands revealed the same fluorescent profile inside cells with dots and filaments, suggesting that the pattern observed is not structure-dependent. Cy5-labeled structures and oligonucleotides gave signal distribution similar to that of Cy3-labeled structures (Figure S4). To gain more insight into the fate of these structures inside cells, we investigated in which organelles the structures are accumulating.

Colocalization Analysis Revealed Mitochondrial Accumulation. Positively charged lipophilic dyes are known to enter the mitochondria due to electrostatic interactions with the mitochondrial membrane.[32] 3,3′-Dihexyloxacarbocyanine iodide (DiOC6), cyanine dyes, and some Alexa dyes can be used to stain the mitochondria. Oligonucleotides labeled with Cy5 or Cy3 have been previously reported as mitochondrial markers in different cell lines, resulting in long filamentous fluorescent signal.[33,34] Therefore, we tested whether our structures can accumulate in the mitochondria and used CellLight Mitochondria-GFP (BacMam 2.0) and CellLight Lysosomes-GFP (BacMam 2.0) to stain the two organelles (Figure S12). The BacMam constructs are plasmids encoding for proteins of the membrane of the organelles fused to Green Fluorescent Protein. One cube clip, the DNA nanocube, and

the DNA tetrahedron were tested (Figure 3 and Figures S13−S18). Colocalization analysis, achieved by measuring the Pearson's coefficients (PCCs) and Mander's coefficients (MCCs), revealed partial colocalization with lysosomes and the mitochondria.[35] For the mitochondria, the structures gave similar PCCs ranging from 0.4 to 0.5 after 4 h incubation and 0.6−0.8 after 24 h incubation. The increase over time suggests slow accumulation in this organelle. The partial colocalization with the lysosome (PCC remains around 0.5−0.6) is consistent with previous reports in the literature, indicating uptake of cyanine dyes, oligos, and structures via endosome/lysosome pathways (Figures S16−S18).[16,36,37]

While cyanine-labeled oligonucleotides have been reported to result in mitochondrial fluorescence signals, finding DNA nanostructures within the mitochondria was surprising and had never been reported previously in the literature. As pointed out by Bao et al. when they studied Cy3-labeled short oligonucleotides, the positive charge of the dye should be largely compensated by the negative charge of the DNA.[33] This makes an entire DNA strand, and to a larger extent a DNA nanostructure, unlikely to interact with the negatively charged mitochondrial membranes. However, the results were the same for the component strands and DNA structures. This may imply that the overall charge of the molecules does not impact accumulation to the mitochondria. Another hypothesis is that the fluorescent signal may simply arise from degradation of the DNA structure with release of the cyanine dye, which is known to cross to the mitochondrial membranes. We decided to investigate whether the fluorescent degradation products, i.e., the cyanine dye being cleaved from the oligo, can cross the cellular membrane and stain the mitochondria. Typically, previous studies have used commercially available versions of the cyanine dye as controls.[34]

Phosphorylated Small-Molecule Cyanine Dyes Colocalize with Nanostructures. Upon recognition by exonucleases and subsequent hydrolysis of the phosphate linkage, two fluorescent degradation products may be produced from cyanine-labeled oligonucleotides: Cy3-phosphate and Cy3-hydroxyl (Figure S19). The Cy3-hydroxyl is positively charged, has almost the same structure than the Cy3 molecule, and is already known as a mitochondrial marker.[33] The Cy3-phosphate carries at least one negative charge (phosphoester pK_{a1} ∼1) that will neutralize the positive charge of the dye. To our knowledge, its interaction with and within cells remains unknown. Therefore, we synthesized Cy3-phosphate (Cy3-P) and Cy5-phosphate (Cy5-P) (Figure 4A and Supporting Information). Fluorescence spectra reveal emission peaks for these molecules similar to those for Cy3 and Cy5 dyes, as well as similar binding to serum proteins in the cellular media (Figures S22 and S23). The dyes have a lower fluorescence
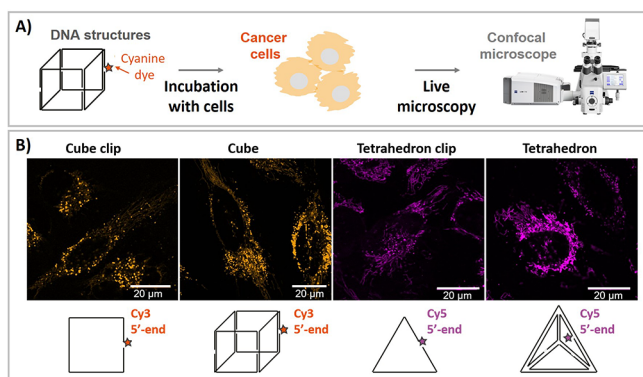

Figure 2. Uptake of DNA oligonucleotides and DNA nanostructures. (A) Experimental setup: DNA structures are incubated with mammalian cells, directly in the cellular media (FBS-supplemented). Fluorescent signal is detected with confocal microscopy. (Microscope image credit: Zeiss Microscopy) (B) After 6 h incubation with HeLa cells, we observed the same fluorescent signal for each DNA nanostructures and their component clip, using live confocal microscopy. Representative images are shown in the figure. Scale bars are 20 μm.
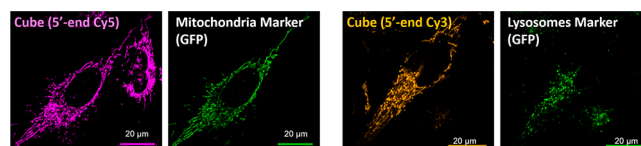

Figure 3. Mitochondrial and lysosomal localization of DNA structures. Live confocal microscopy in HeLa cells revealed colocalization of DNA structures. In the image, we represent the Cy5-labeled DNA nanocube colocalizing with mitochondria and the Cy3-labeled DNA nanocube with the lysosomes, both after 24 h incubation. Representative images are shown in the figure.
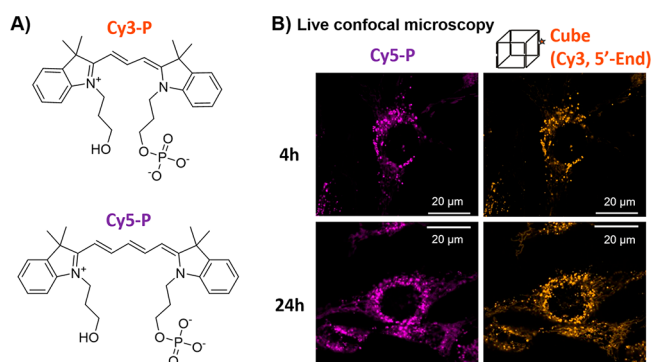
Figure 4. Phosphorylated dyes colocalize with DNA structures. (A) Structures of synthesized phosphorylated cyanine 3 (Cy3-P) and cyanine 5 (Cy5-P) dyes. (B) Co-incubation of structures and model for degradation products (free dyes) revealed high colocalization, using live confocal microscopy in HeLa cells. Representative images are shown in the figure.

intensity compared to the DNA-labeled strands (Figures S82 and S83). Indeed, attaching these fluorophores to DNA likely increased the local viscosity resulting in higher fluorescence emission.[38]

We then incubated the dyes with HeLa cells in FBS-containing media (1.5 h, 6 h, 24 h). Dyes were taken up quickly (less than 1.5 h) and gave the exact same filamentous signal with some bright spots as dye-labeled DNA strands (Figures S24 and S25). Partial colocalization with mitochondria (Cy5-P) and lysosomes (Cy3-P and Cy5-P) was measured and showed results similar to those obtained with oligonucleotides and DNA structures (Figures S26–S28). Co-incubating the two dyes Cy3-P and Cy5-P with cells resulted in complete colocalization of their respective signals (PCC is ranging from 0.85 to 0.95). (Figure S29). Interestingly, upon co-incubation, *each of our previously tested oligonucleotides and nanostructures was found to colocalize with the dye* (Figure 4B and Figures S30–S35). Finally, we tested the cellular uptake of the Cy3-

labeled dinucleotide (Cy3-TG), another model for DNA degradation as it should lead to both potential degradation products quickly (Cy3-phosphate and Cy3-hydroxyl). Cy3-TG strongly colocalized with the Cy5-P signal. (Figure S36).

In brief, our degradation model compounds for cyanine-labeled DNA strands (the phosphorylated dyes) colocalize with DNA structures. This suggests that the intracellular fluorescent signal may be caused by the degradation product entering the cell, i.e., the dye getting cleaved from the DNA, and not by uptake of the DNA structure. Therefore, it favors the degradation hypothesis over the hypothesis of the dye guiding the entire structure to the mitochondria. To confirm this, we looked at uptake kinetics and synthesized structures that are more resistant to nuclease degradation. These structures will lead to a slower release of the cyanine dye within the cell media, potentially allowing the DNA structure to enter cells before its degradation by nucleases.

More-Resistant DNA Cubes and Clip Components Result in Slower Intracellular Fluorescence. When we examined the kinetics of cellular uptake, we noted that the free dyes and the free dinucleotide Cy3-TG were taken up in less than 2 h. Intracellular fluorescence from the 5′-end labeled clip appears and increases after 2 h, while it takes more than 4 h for the 3D structures to give a detectable signal (Figure S9). At 24 h, the signal from the clip and the structures are the same. Similar results were observed by Bao et al. as they studied different length oligonucleotides.[33] We hypothesize that the delayed signal is caused by a delayed degradation. Indeed, DNA 3D constructs are more stable than their single-stranded components.[7] Therefore, as it takes more time for nucleases to digest the strand and for the dye to get cleaved, the fluorescence signal is delayed. To test this hypothesis, we synthesized new structures with different serum stabilities, resulting in different release rates of the cyanine dye.

In serum, 3′-exonucleases are the main cause for DNA degradation, while inside the cell both 5′- and 3′-exonucleases will degrade oligonucleotides.[39,40] Therefore, labeling the strand on the 5′-end does not protect it from the main source
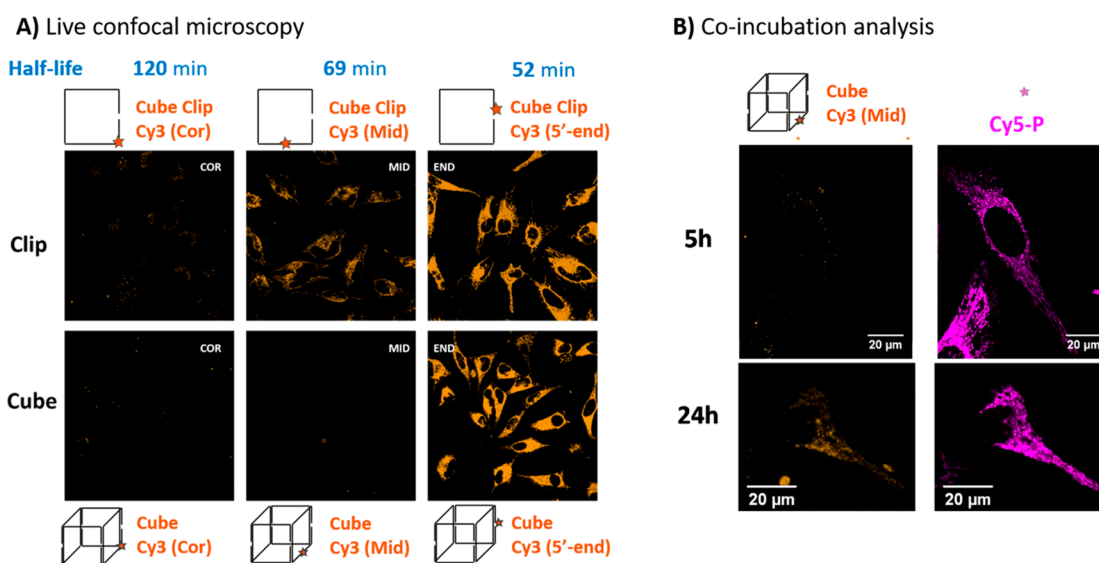

Figure 5. Changing the dye position within the structure. Representative images are shown in the figure. (A) Live confocal microscopy of HeLa cells (24 h incubation) with the different clips and cubes at fixed laser settings. The experiment revealed that release of the dye at later time points caused a delay in the appearance of the fluorescent signal. (B) Co-incubation with the phosphorylated dye confirmed colocalization of the more stable structures with this model for degradation products.
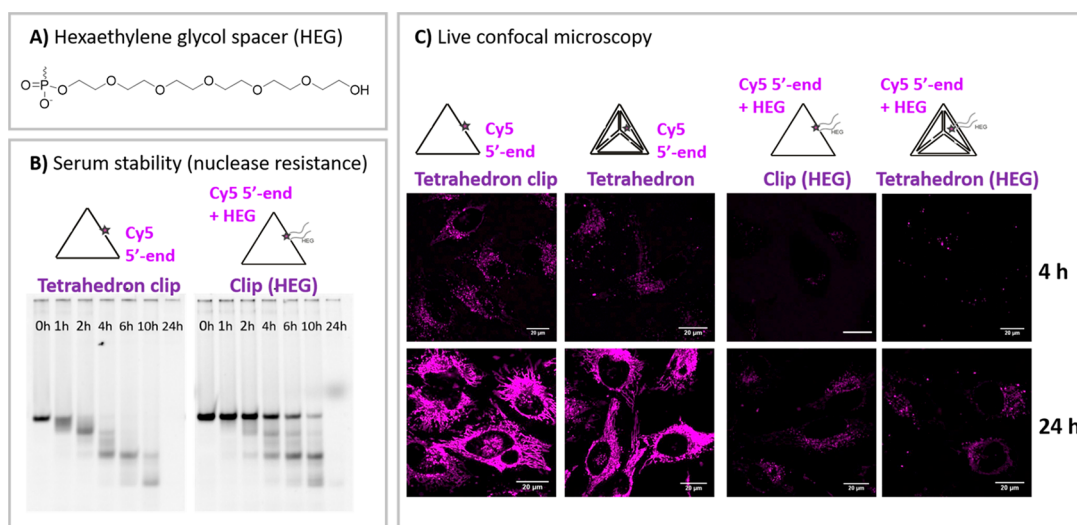
Figure 6. HEG-protection of the DNA tetrahedron. (A) Chemical structure of HEG modification. (B) Gel electrophoresis from serum stability experiments. The component clip of the tetrahedron revealed higher stability of the clip component upon HEG-labeling at 5′- and 3′-ends. Cy5 channel is displayed. (C) Live confocal microscopy (HeLa cells, fixed laser settings) revealed that the more stable structures caused a delayed cellular uptake. Scale bars at 20 μm. Representative images are shown in the figure.

of nuclease degradation in cell media, leading to a fast release of the dye. To overcome this stability issue, we synthesized cube clips with Cy3 and Cy5 positioned at the 3′-end. We also synthesized two DNA clips with the dye "buried" in the sequence by changing the position to two different internal positions: one at the corner of the cube structure (Clip "Cor"), and one in the single-stranded region (Clip "Mid") (Figure 5A and Table S-I). To verify increased nuclease resistance, we performed serum stability experiments: strands were mixed in cell media (supplemented with serum, that contains nucleases), samples were collected at different time points and analyzed using gel electrophoresis experiments. The half-life extracted from these experiments reflect the time at which 50% of the full product is still intact, but it does not give us the exact time of release of the phosphorylated dye degradation product (Cy3-P or Cy5-P). It is still, however, a good indication of the relative stabilities of each of the strands.

The half-life of the clip with Cy3 positioned at the 5′-end is the shortest (52 min), and the 3′-modification dramatically increased the resistance to extracellular enzymes (236 min). The two internal positions also increased serum stability but gave different results (69 min (mid) and 120 min (cor)) (Figures S37 and S38 and Table S-II), most likely due to sequence dependence of nuclease activity.[41] The assembled DNA cubes have higher stabilities than the clip counterparts (Table S-III). The different modifications only slightly affected the overall stability of the cube structure (Figures S41 and S42). In denaturing conditions of the self-assembled structures, the 3′-end and the corner modification still have the highest stabilities, meaning that the dye from these structures should be released last (Figures S43 and S44).

We incubated the different clips and structures with HeLa cells and looked at the fluorescent signal using confocal live microscopy (Figures S53−S64). After 4−5 h incubation, the uptake of the more stable clips or structures is barely detectable while the 5′-end clip gives a strong fluorescent signal. When comparing the intracellular fluorescence, by fixing the laser settings, the signal of the 5′-end labeled strands and cubes seems much higher than for the other clips (Figure 5A

and Figure S65). We believe that this difference in intracellular fluorescence is caused by the slower degradation of the strands, causing delayed signal. Indeed, at 24 h, our serum stability experiments revealed that the 5′-end labeled strand is fully degraded while a smearing on the gel can be observed for the other strands (3′-, cor, and mid), indicating the presence of a variety of different length oligonucleotides (Figure S37). Finally, we co-incubated the phosphorylated dyes with the different constructs and confirmed the colocalization of the signal for all the DNA structures at 24 h, by measuring the PCCs and MCCs (Figure 5B and Figures S53−S64).

In short, as we slow down degradation and dye release, the signal appears slower for cube clips and cubes, strengthening the hypothesis of degradation of the structure followed by cellular uptake of the dye (or short dye-labeled oligonucleotides). Results were confirmed in another cancer cell line, HepG2 cells (liver hepatocellular cells). We observed cellular uptake of the dyes and delayed uptake of the 3′-end labeled structure. (Figures S94−S98). To confirm further that stable structures are taken up later, we looked at the DNA tetrahedron, which is fully double-stranded and more resistant to nucleases.

Hexaethylene Glycol To Prevent DNA Tetrahedron Degradation. The tetrahedron structure has been extensively investigated in biological studies.[17] However, in our hands, the assembly of the tetrahedron led to multiple higher mobility products in the gel, indicating the formation of higher-order assemblies (Figure S1).[42,43] We used this mix of products for our studies, as the protocol has been widely used by the community (Supporting Information).[17,44] We also purified the tetrahedron structure using electrophoretic methods, to further confirm our results with the monodisperse structure (Figure S1).

To prevent the release of the dye, we synthesized a fluorescently labeled clip protected by hexaethylene glycol units (HEG) at both the 3′- and 5′-ends. The HEG modification increased resistance to nuclease degradation (Figures S39 and S40, and Tables S2 and S3). The modification did not affect the overall stability of the

tetrahedron, but the clip from the structure is more stable (Figures S45, S46, S48, and S49). Incubation with cells led to similar conclusions: the HEG protection, as it increased the nuclease resistance, significantly delayed the cellular uptake (Figure 6 and Figures S67 and S68). Co-incubation of Cy3-P with tetrahedron, purified tetrahedron, and HEG-protected tetrahedron confirmed colocalization with the degradation product (Figures S66−S72). Results were confirmed in HepG2 cell line as well (Figures S99−S102).

At early time points (4 h), we observed very faint dots (laser power and gain were increased) from the DNA structure that do not colocalize with the dye (Figures S67 and S68), possibly due to very low uptake of intact structures or oligos, consistent with the 1−2% uptake observed by Turberfield et al.[15] These strands eventually degrade after cellular uptake (endosomal pH and cytoplasmic nucleases), releasing the dye as well. All these experiments indicate that as we stabilize the dye-labeled DNA strand, the fluorescent signal is simply delayed. We then investigated other methods to prevent DNA degradation and dye uptake, such as changing serum conditions or using negatively charged fluorescent dyes, to further assess the serum degradation hypothesis.

Changing Serum Conditions To Prevent DNA Degradation. To prevent extracellular nuclease degradation, we tested uptake in low-serum conditions (0.1% FBS instead of 10%). At 0.1% FBS concentration, nuclease degradation should be dramatically reduced. We did observe uptake of the free dyes; however, uptake of 5′-end-labeled clip and cube, as well as of the 3′-end-labeled clips, was considerably reduced (Figure 7A and Figures S73−S75). This seems to indicate that our DNA constructs need to be degraded to produce a detectable signal. We also performed "pulse-chase" experiments where structures are incubated in serum-free conditions (0% FBS) for 15−20 min, cells are washed, and new cell culture media (10% FBS) is then added.[45] Much lower signal could be detected, and after 1 day incubation, we did observe the same pattern than for degraded products (filament and dots) (Figure S76). More stable structures gave a delayed signal compared to less stable ones (3′- vs 5′-Cy3 cubes), suggesting uptake of the degraded product (Figure S77). Curiously, this result suggests binding or low uptake of some structures into the cell, which are not washed away by the washing steps and are eventually getting degraded.

Sulfonated Cyanine Dyes Do Not Accumulate in the Mitochondria. Negatively charged sulfonate groups are typically placed on cyanine dyes to increase their solubility in water, avoid dye aggregation, and prevent their cellular uptake.[46] We used click chemistry and one of our previously developed phosphoramidites to label the cube clip with a sulfonated Cy5 at its 5′-end or in an internal position (Figure 7B and Figures S91 and S92).[47] The sulfonated clip and cube gave little fluorescent signal inside cells compared to the non-sulfonated Cy5 (Figure 7C and Figure S93). This means that the intracellular fluorescence is dye-dependent and that low fluorescent signal, sometimes observed from other dyes can not be correlated with uptake of the structure. We believe that the observation of a fluorescent signal should always be followed by a quantification of the uptake. For example, quantification methods such as streptavidin−biotin labeling or qPCR methods revealed low uptake of nanostructures inside cells.[16,48]

In conclusion, all our experiments are consistent with prior degradation of the cyanine-labeled dye, followed by uptake of
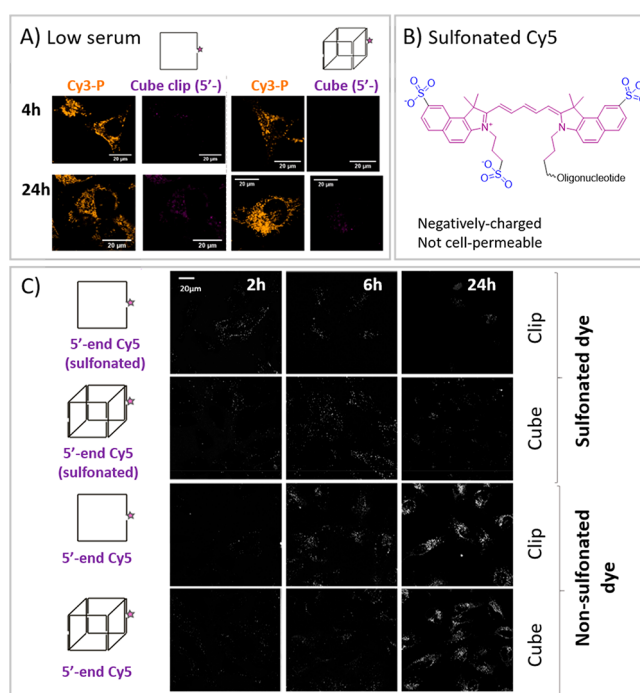

Figure 7. Lowering serum conditions and changing the dye to its sulfonated version. Representative images are shown in the figure. (A) Live confocal microscopy in HeLa cells in low-serum conditions (0.1% FBS) revealed that with reduced degradation, no fluorescent signal is observed. (B) Chemical structure of sulfonated Cy5 dye, negatively charged. (C) Structures labeled with sulfonated dye did not produce any intracellular fluorescent signal compared to non-sulfonated labeled structures.

the fluorescent dye inside the cell, leading to most of the observed fluorescent signal. Previous research from various laboratories has indicated uptake of DNA nanostructures through endosomal pathways and used FRET experiments to prove their integrity inside cells. These results are in apparent contradiction with our observations, and we therefore examined FRET experimental design in more details.

Free Dyes Cy3-P and Cy5-P Can Give an Intracellular FRET Signal. DNA structures can easily be labeled with a FRET pair, for example Cy3/Cy5.[15,49] Precisely two components strands are labeled: one with Cy3 (donor), one with Cy5 (acceptor), such that the two dyes are close enough (1−10 nm) to allow energy transfer upon excitation of Cy3. If the structure is disassembled, no energy transfer will happen. Therefore, the observation of FRET signal intracellularly is in general explained by invoking the uptake of an intact structure. As shown above, we observed that the two free dyes highly colocalize in cells (Figure S29). We believe this is due to their high local concentration in the lysosome and their accumulation in the mitochondria. We decided to test whether these two separate dye molecules can give a FRET signal inside live cells, giving rise to an "incorrect FRET signal" (sometimes called *random FRET*).[50] We synthesized a positive control for FRET: a DNA strand labeled with Cy3 and Cy5 directly attached to one another via a phosphodiester bond at the 5′-end called *strand Cy3-Cy5* (Table S-I). Emission spectra confirmed that the strand Cy3-Cy5 causes FRET emission in DMEM (cell media) and FBS-supplemented DMEM, while no signal was observed for the free dyes or for mixture of dyes with labeled DNA strands (Figures S82−S84). The Cy3-Cy5
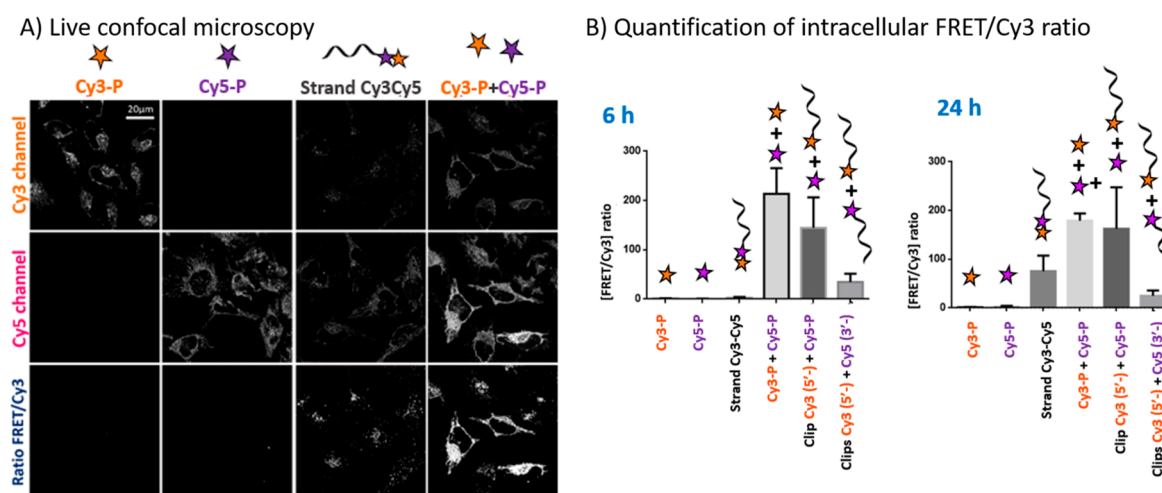
Figure 8. Förster resonance energy transfer (FRET) experiments. (A) Live confocal microscopy after 24 h incubation in HeLa cells. Representative images are shown in the figure. (B) Quantification of the gray level intensity from the microscopy experiments (detailed protocols in the Supporting Information). These two experiments revealed that the two free separate small molecules can give a FRET signal, even though they are not in close proximity before incubation.

phosphate bond in the strand Cy3-Cy5 remains stable upon addition of serum (Figure S85), confirming it can be used as a positive control.

We then examined FRET signals in live cells at 6 and 24 h, using confocal microscopy. Structures and dyes were incubated at 150 nM final concentration. After background and cross-talk corrections, we calculated the FRET/Cy3 ratio to quantify energy transfer.[51] *Surprisingly, we observed high FRET signal when the two free phosphorylated dyes Cy3-P and Cy5-P were co-incubated*, while the FRET-positive strand gave a smaller signal (Figure 8 and Figures S88−S90). At 6 h, the ratio is high for the two co-incubated dyes and for the 5′-end-labeled clip co-incubated with free dye. The positive control, the strand Cy3-Cy5, gives almost no signal. We believe full DNA degradation was not reached at this time point and that the linked dyes from the degraded DNA strand had not yet entered the cell to a high extent (Figure S85). At 24 h, the strand Cy3-Cy5 gives a small signal, less than that of the two free dyes. *Interestingly, co-incubating a Cy3-labeled DNA strand (5′-end, less stable) with a separate Cy5-labeled DNA strand (3′-end, more stable) resulted in a measurable FRET/Cy3 ratio, albeit lower than the two free dyes, consistent with the degradation hypothesis.* Overall, the fact that we can observe *random* FRET signal with two separate small-molecule dyes supports the need of carefully designed controls for FRET experiments with DNA strands and structures. The signals from the free dyes should be studied, or two chemically different dyes should be used.

Fluorescent Signal Is Washed Away by Chemical Fixation. Another important parameter to compare our work to other studies in the literature is the use of live confocal microscopy to prevent effects from the fixative agents on the fluorescent signal. Cyanine dye accumulation inside the mitochondria does not resist chemical fixative agents like formaldehyde.[32] We tested whether the signal is disrupted by chemical fixation. When we fixed cells with formaldehyde, the filamentous signal of the phosphorylated dyes disappeared, and we saw only bright dots (endosome/lysosomes) and diffuse cytoplasmic signal (Figure S78). The result was similar for oligonucleotides (Figure S79), but Cy3-P and Cy5-P still colocalized (Figure S80). Methanol fixation removed all the

fluorescent signal or caused DNA precipitation (Figure S81). This emphasizes that the effect of chemical fixation needs to be carefully studied since it can cause misleading information.

Safety Statement. No unexpected or unusually high safety hazards were encountered in the course of this work.

3. CONCLUSION

The observation of colocalized signals when DNA structures and their degradation products are administered to cells indicates that intracellular fluorescence does not necessarily correlate with cellular uptake. Instead, experiments revealed that most of the signal arises from degradation of DNA structures by nucleases, releasing the fluorescent dye that is then taken up inside cells. In particular, we observed that, as we stabilized the dye within the structure, uptake was delayed. Changing the dye to its cell-impermeable version (sulfonated) or preventing serum degradation considerably reduced the intracellular fluorescence. Interestingly, FRET signals were observed between the separate free cyanine dyes inside cells, revealing the need for more carefully designed controls when using FRET experiments to assess uptake of intact DNA structures. Protocol design, such as the use of chemical fixation instead of live conditions, can also dramatically change the pattern of the fluorescence signal.

In this study, we focused on wireframe DNA-minimal architectures. However, we believe that the findings can be extended to any nucleic acid-based material, such as DNA origami or RNA therapeutics, as nucleases can still access and degrade the labeled strands. DNA-dense structures such as DNA origami may have different degradation profiles than wireframe structures, but they are still prone to nuclease degradation within a few hours and disassembly as the dication concentration is lower in biological media.[52] The fluorescent dye to track DNA origami cellular uptake is often placed at the 5′- or 3′-end of the short staple strands and can protrude from the surface of the origami.[53] Embedding the dye within the structure was shown to result in a longer stability of the FRET signal, coherent with longer structural integrity.[54]

Beside the signal from the degradation product, the fluorescence signal and intensity will depend on many

parameters linked to the nature of the dye: binding to serum proteins can increase fluorescence, as can sequence-specific attachment to a DNA strand.[46,55] Cellular localization is known to influence the brightness of the dye, for example because of changes of pH in the different organelles.[56] Therefore, altered fluorescence intensity could simply arise from longer retention in the endosomal compartment, where the dye may be brighter or dimmer (lowed pH). We believe that measuring the total fluorescence intensity in a cell, for example by using flow cytometry, cannot be simply correlated with higher uptake of a structure. Precise colocalization and fluorescence analysis need to be performed.

Furthermore, our results may indicate that cyanine dyes may not be an ideal choice for the investigation of cellular uptake of DNA structures. Cyanine dyes fluorescence is strongly dependent on its local environment.[38] On the other hand, the cell permeability of the cyanine dyes allowed us to detect the uptake of the degradation products inside the cell. It is important to note, however, that using other types of dyes would not prevent the fluorescent molecule from getting cleaved off the DNA strand; they would simply change the intensity or location of the intracellular fluorescent signal arising from degradation. The absence of a signal can be difficult to study, as it could just indicate issues with the experimental setup. Overall, we believe that, in addition to choosing the dye carefully, control experiments involving a *phosphorylated free dye* as a model of degradation, rather than only unsubstituted dye, should be systematically performed when using fluorescence methods such as microscopy, flow cytometry, or FRET. Two chemically different dyes can be used to confirm that the results observed are not dye-dependent.

Thorough quantification of the uptake of the DNA structure is also needed if the structure is thought to enter the cell. Non-fluorescent methods such as gene silencing experiments, qPCR, or biotin-labeling can be used for quantification. Overall, our results can be used as a cautionary tale on how to design and analyze fluorescence experiments when examining the uptake profile of DNA-based materials. For fluorescence-based assays, we recommend (a) comparison of uptake with model of degradation products (such as the phosphorylated dye, even for FRET experiments), (b) correlation of degradation kinetics with cellular uptake kinetics, (c) thorough controls and optimization of the cellular work conditions (serum, fixation, temperature), and (d) changing the nature and position of the dye to track whether the signal is dye-dependent or not (and trying to place the dye in less accessible positions on the labeled oligonucleotide).

Finally, our findings bring new important considerations for the use of DNA nanostructures in biological systems. First, we believe that our results may not be contradictory with previously reported successful examples of DNA nanostructures inside cells, but instead they provide clues on the design of more reliable fluorescence-based assays. We hope they will help the community deciphering the rules that govern the successful uptake of certain DNA structures compared to others.

We also believe that revealing that wireframe DNA nanostructures do not enter cells to a high extent can be turned into a real advantage in using them as drug delivery devices. Nonspecific cellular uptake of DNA cages is not desirable, as it would mean that cages can penetrate different cells *in vivo*. Instead, it gives us the opportunity to attach targeting ligands on these cages to promote their entry into specific cells—for example, folate decoration can lead to internalization into cancer cells.[25] To increase cellular uptake, inspiration can also be taken from the extensive work done by the oligonucleotide therapeutics field. Specifically, we believe that inserting chemical modifications in DNA (nucleobase, backbone, 3'- and 5'-end modifications) could reduce nuclease degradation while substantially increasing uptake of DNA cages.[57] On the other hand, because of their poor uptake, DNA nanostructures could be used as biosensors or bioimaging systems outside of the cell.[27,28] Their programmability and higher nuclease resistance compared to single-stranded DNA make them excellent biodegradable materials to sense the cell surface or extracellular proteins. They could also be used to promote cell−cell interaction, by targeting membrane receptors.[58] Finally, as drug delivery systems, they could also be designed to carry small-molecule drugs. The DNA cage degradation could lead to a slow release of the drug that can then be internalized by the targeted cells. Stabilizing the structure, to control the rate of drug release, can be achieved by the introduction of chemical modifications in the bases or the DNA backbone, chemical coating, or binding to serum proteins.[9,54,59]

■ ASSOCIATED CONTENT

Ⓢ Supporting Information

The Supporting Information is available free of charge on the ACS Publications website at DOI: 10.1021/acscentsci.9b00174.

> General protocols and instrumentation information, DNA strands and structures synthesis and characterization, live confocal microscopy images (cellular uptake of dyes, oligonucleotides, and structures) and colocalization analysis, serum stability assays, serum-free experiments, analysis of effect of fixating agents, FRET experiments, fluorescence spectra, sulfonated dyes synthesis and uptake, and results in HepG2 cell line, including Figures S1−S102 and Tables S-I−S-III (PDF)

■ AUTHOR INFORMATION

Corresponding Author
*E-mail: hanadi.sleiman@mcgill.ca.
ORCID Ⓞ
Hanadi F. Sleiman: 0000-0002-5100-0532
Notes
The authors declare no competing financial interest.

■ ACKNOWLEDGMENTS

■ REFERENCES

(1) Juliano, R. L. The delivery of therapeutic oligonucleotides. *Nucleic Acids Res.* **2016**, *44* (14), 6518−6548.

(2) Chen, Y.-J.; Groves, B.; Muscat, R. A.; Seelig, G. DNA nanotechnology from the test tube to the cell. *Nat. Nanotechnol.* **2015**, *10* (9), 748−760.

(3) Crooke, S. T.; Wang, S.; Vickers, T. A.; Shen, W.; Liang, X.-h. Cellular uptake and trafficking of antisense oligonucleotides. *Nat. Biotechnol.* **2017**, *35*, 230−237.

(4) Cutler, J. I.; Auyeung, E.; Mirkin, C. A. Spherical nucleic acids. *J. Am. Chem. Soc.* **2012**, *134* (3), 1376−1391.

(5) Seeman, N. C.; Sleiman, H. F. DNA nanotechnology. *Nature Reviews Materials.* **2017**, *3*, 17068.

(6) Bujold, K. E.; Lacroix, A.; Sleiman, H. F. DNA nanostructures at the interface with biology. *Chem.* **2018**, *4* (3), 495−521.

(7) Conway, J. W.; McLaughlin, C. K.; Castor, K. J.; Sleiman, H. DNA nanostructure serum stability: greater than the sum of its parts. *Chem. Commun.* **2013**, *49* (12), 1172−1174.

(8) Edwardson, T. G.; Carneiro, K. M.; McLaughlin, C. K.; Serpell, C. J.; Sleiman, H. F. Site-specific positioning of dendritic alkyl chains on DNA cages enables their geometry-dependent self-assembly. *Nat. Chem.* **2013**, *5* (10), 868−875.

(9) Lacroix, A.; Edwardson, T. G.; Hancock, M.; Dore, M.; Sleiman, H. F. Development of DNA nanostructures for high-affinity binding to human serum albumin. *J. Am. Chem. Soc.* **2017**, *139* (21), 7355−7362.

(10) Fakhoury, J. J.; McLaughlin, C. K.; Edwardson, T. W.; Conway, J. W.; Sleiman, H. F. Development and characterization of gene silencing DNA cages. *Biomacromolecules* **2014**, *15* (1), 276−282.

(11) Bujold, K. E.; Fakhoury, J.; Edwardson, T. G. W.; Carneiro, K. M. M.; Briard, J. N.; Godin, A. G.; Amrein, L.; Hamblin, G. D.; Panasci, L. C.; Wiseman, P. W.; Sleiman, H. F. Sequence-responsive unzipping DNA cubes with tunable cellular uptake profiles. *Chem. Sci.* **2014**, *5* (6), 2449−2455.

(12) Liu, Z.; Li, Y.; Tian, C.; Mao, C. A smart DNA tetrahedron that isothermally assembles or dissociates in response to the solution pH value changes. *Biomacromolecules* **2013**, *14* (6), 1711−1714.

(13) Yang, Y.; Endo, M.; Hidaka, K.; Sugiyama, H. Photo-controllable DNA origami nanostructures assembling into prede-signed multiorientational patterns. *J. Am. Chem. Soc.* **2012**, *134* (51), 20645−20653.

(14) Ding, H.; Li, J.; Chen, N.; Hu, X.; Yang, X.; Guo, L.; Li, Q.; Zuo, X.; Wang, L.; Ma, Y.; Fan, C. DNA nanostructure-programmed like-charge attraction at the cell-membrane interface. *ACS Cent. Sci.* **2018**, *4* (10), 1344−1351.

(15) Walsh, A. S.; Yin, H.; Erben, C. M.; Wood, M. J. A.; Turberfield, A. J. DNA cage delivery to mammalian cells. *ACS Nano* **2011**, *5* (7), 5427−5432.

(16) Vindigni, G.; Raniolo, S.; Ottaviani, A.; Falconi, M.; Franch, O.; Knudsen, B. R.; Desideri, A.; Biocca, S. Receptor-mediated entry of pristine octahedral DNA nanocages in mammalian cells. *ACS Nano* **2016**, *10* (6), 5971−5979.

(17) Xie, N.; Liu, S.; Yang, X.; He, X.; Huang, J.; Wang, K. DNA tetrahedron nanostructures for biological applications: biosensors and drug delivery. *Analyst* **2017**, *142*, 3322−3332.

(18) Kim, K.-R.; Lee, Y.-D.; Lee, T.; Kim, B.-S.; Kim, S.; Ahn, D.-R. Sentinel lymph node imaging by a fluorescently labeled DNA tetrahedron. *Biomaterials* **2013**, *34* (21), 5226−5235.

(19) Lee, D. S.; Qian, H.; Tay, C. Y.; Leong, D. T. Cellular processing and destinies of artificial DNA nanostructures. *Chem. Soc. Rev.* **2016**, *45* (15), 4199−4225.

(20) Keum, J.-W.; Ahn, J.-H.; Bermudez, H. Design, assembly, and activity of antisense DNA nanostructures. *Small* **2011**, *7* (24), 3529−3535.

(21) Charoenphol, P.; Bermudez, H. Aptamer-targeted DNA nanostructures for therapeutic delivery. *Mol. Pharmaceutics* **2014**, *11* (5), 1721−1725.

(22) Xia, Z.; Wang, P.; Liu, X.; Liu, T.; Yan, Y.; Yan, J.; Zhong, J.; Sun, G.; He, D. Tumor-penetrating peptide-modified DNA tetrahedron for targeting drug delivery. *Biochemistry* **2016**, *55* (9), 1326−1331.

(23) Wang, P.; Rahman, M. A.; Zhao, Z.; Weiss, K.; Zhang, C.; Chen, Z.; Hurwitz, S. J.; Chen, Z. G.; Shin, D. M.; Ke, Y. Visualization of the cellular uptake and trafficking of DNA origami nanostructures in cancer cells. *J. Am. Chem. Soc.* **2018**, *140* (7), 2478−2484.

(24) Bastings, M. M. C.; Anastassacos, F. M.; Ponnuswamy, N.; Leifer, F. G.; Cuneo, G.; Lin, C.; Ingber, D. E.; Ryu, J. H.; Shih, W. M. Modulation of the cellular uptake of DNA origami through control over mass and shape. *Nano Lett.* **2018**, *18* (6), 3557−3564.

(25) Lee, H.; Lytton-Jean, A. K. R.; Chen, Y.; Love, K. T.; Park, A. I.; Karagiannis, E. D.; Sehgal, A.; Querbes, W.; Zurenko, C. S.; Jayaraman, M.; Peng, C. G.; Charisse, K.; Borodovsky, A.; Manoharan, M.; Donahoe, J. S.; Truelove, J.; Nahrendorf, M.; Langer, R.; Anderson, D. G. Molecularly self-assembled nucleic acid nanoparticles for targeted in vivo siRNA delivery. *Nat. Nanotechnol.* **2012**, *7*, 389.

(26) Bhatia, D.; Surana, S.; Chakraborty, S.; Koushika, S. P.; Krishnan, Y. A synthetic icosahedral DNA-based host-cargo complex for functional in vivo imaging. *Nat. Commun.* **2011**, *2*, 339.

(27) Douglas, S. M.; Bachelet, I.; Church, G. M. A logic-gated nanorobot for targeted transport of molecular payloads. *Science* **2012**, *335* (6070), 831−834.

(28) Li, S.; Jiang, Q.; Liu, S.; Zhang, Y.; Tian, Y.; Song, C.; Wang, J.; Zou, Y.; Anderson, G. J.; Han, J.-Y.; Chang, Y.; Liu, Y.; Zhang, C.; Chen, L.; Zhou, G.; Nie, G.; Yan, H.; Ding, B.; Zhao, Y. A DNA nanorobot functions as a cancer therapeutic in response to a molecular trigger in vivo. *Nat. Biotechnol.* **2018**, *36*, 258−264.

(29) Hughes, L. D.; Rawle, R. J.; Boxer, S. G. Choose your label wisely: water-soluble fluorophores often interact with lipid bilayers. *PLoS One* **2014**, *9* (2), No. e87649.

(30) Zhu, H.; Fan, J.; Du, J.; Peng, X. Fluorescent probes for sensing and imaging within specific cellular organelles. *Acc. Chem. Res.* **2016**, *49* (10), 2115−2126.

(31) Xu, W.; Zeng, Z.; Jiang, J.-H.; Chang, Y.-T.; Yuan, L. Discerning the chemistry in individual organelles with small-molecule fluorescent probes. *Angew. Chem., Int. Ed.* **2016**, *55* (44), 13658−13699.

(32) Macho, A.; Decaudin, D.; Castedo, M.; Hirsch, T.; Susin, S. A.; Zamzami, N.; Kroemer, G. Chloromethyl-X-rosamine is an aldehyde-fixable potential-sensitive fluorochrome for the detection of early apoptosis. *Cytometry* **1996**, *25* (4), 333−340.

(33) Rhee, W. J.; Bao, G. Slow non-specific accumulation of 2'-deoxy and 2'-O-methyl oligonucleotide probes at mitochondria in live cells. *Nucleic Acids Res.* **2010**, *38* (9), No. e109.

(34) Lorenz, S.; Tomcin, S.; Mailänder, V. Staining of mitochondria with Cy5-labeled oligonucleotides for long-term microscopy studies. *Microsc. Microanal.* **2011**, *17* (3), 440−445.

(35) Bolte, S.; Cordelières, F. P. A guided tour into subcellular colocalization analysis in light microscopy. *J. Microsc.* **2006**, *224* (3), 213−232.

(36) Liang, L.; Li, J.; Li, Q.; Huang, Q.; Shi, J.; Yan, H.; Fan, C. Single-particle tracking and modulation of cell entry pathways of a tetrahedral DNA nanostructure in live cells. *Angew. Chem., Int. Ed.* **2014**, *53* (30), 7745−7750.

(37) Surana, S.; Bhat, J. M.; Koushika, S. P.; Krishnan, Y. An autonomous DNA nanomachine maps spatiotemporal pH changes in a multicellular living organism. *Nat. Commun.* **2011**, *2*, 340.

(38) Ha, T.; Tinnefeld, P. Photophysics of fluorescent probes for single-molecule biophysics and super-resolution imaging. *Annu. Rev. Phys. Chem.* **2012**, *63*, 595−617.

(39) Eder, P. S.; DeVine, R. J.; Dagle, J. M.; Walder, J. A. Substrate specificity and kinetics of degradation of antisense oligonucleotides by a 3' exonuclease in plasma. *Antisense Res. Dev.* **1991**, *1* (2), 141−151.

(40) Crooke, R. M.; Graham, M. J.; Martin, M. J.; Lemonidis, K. M.; Wyrzykiewiecz, T.; Cummins, L. L. Metabolism of antisense oligonucleotides in rat liver homogenates. *J. Pharmacol. Exp. Ther.* **2000**, *292* (1), 140−149.

(41) Perkins, T. T.; Dalal, R. V.; Mitsis, P. G.; Block, S. M. Sequence-dependent pausing of single lambda exonuclease molecules. *Science* **2003**, *301* (5641), 1914−1918.

(42) Setyawati, M. I.; Kutty, R. V.; Tay, C. Y.; Yuan, X.; Xie, J.; Leong, D. T. Novel theranostic DNA nanoscaffolds for the simultaneous detection and killing of escherichia coli and staphylococcus aureus. *ACS Appl. Mater. Interfaces* **2014**, *6* (24), 21822− 21831.

(43) Kim, K. R.; Kim, D. R.; Lee, T.; Yhee, J. Y.; Kim, B. S.; Kwon, I. C.; Ahn, D. R. Drug delivery by a self-assembled DNA tetrahedron for overcoming drug resistance in breast cancer cells. *Chem. Commun.* **2013**, *49* (20), 2010−2012.

(44) Goodman, R. P.; Berry, R. M.; Turberfield, A. J. The single-step synthesis of a DNA tetrahedron. *Chem. Commun.* **2004**, No. 12, 1372−1373.

(45) Modi, S.; Xwetha, M. G.; Goswami, D.; Gupta, G. D.; Mayor, S.; Krishnan, Y. A DNA nanomachine that maps spatial and temporal pH changes inside living cells. *Nat. Nanotechnol.* **2009**, *4*, 325−330.

(46) Agbavwe, C.; Somoza, M. M. Sequence-dependent fluorescence of cyanine dyes on microarrays. *PLoS One* **2011**, *6* (7), No. e22177.

(47) de Rochambeau, D.; Sun, Y.; Barlog, M.; Bazzi, H. S.; Sleiman, H. F. Modular strategy to expand the chemical diversity of DNA and sequence-controlled polymers. *J. Org. Chem.* **2018**, *83* (17), 9774− 9786.

(48) Okholm, A. H.; Nielsen, J. S.; Vinther, M.; Sørensen, R. S.; Schaffert, D.; Kjems, J. Quantification of cellular uptake of DNA nanostructures by qPCR. *Methods* **2014**, *67* (2), 193−197.

(49) Bujold, K. E.; Hsu, J. C. C.; Sleiman, H. F. Optimized DNA "nanosuitcases" for encapsulation and conditional release of siRNA. *J. Am. Chem. Soc.* **2016**, *138* (42), 14030−14038.

(50) Vogel, S. S.; Thaler, C.; Koushik, S. V. Fanciful FRET. *Sci. Signaling* **2006**, *2006* (331), No. re2.

(51) Broussard, J. A.; Rappaz, B.; Webb, D. J.; Brown, C. M. Fluorescence resonance energy transfer microscopy as demonstrated by measuring the activation of the serine/threonine kinase Akt. *Nat. Protoc.* **2013**, *8*, 265−281.

(52) Hahn, J.; Wickham, S. F. J.; Shih, W. M.; Perrault, S. D. Addressing the Instability of DNA Nanostructures in Tissue Culture. *ACS Nano* **2014**, *8* (9), 8765−8775.

(53) Rahman, M. A.; Wang, P.; Zhao, Z.; Wang, D.; Nannapaneni, S.; Zhang, C.; Chen, Z.; Griffith, C. C.; Hurwitz, S. J.; Chen, Z. G.; Ke, Y.; Shin, D. M. Systemic Delivery of Bc12-Targeting siRNA by DNA Nanoparticles Suppresses Cancer Cell Growth. *Angew. Chem., Int. Ed.* **2017**, *56* (50), 16023−16027.

(54) Ponnuswamy, N.; Bastings, M. M. C.; Nathwani, B.; Ryu, J. H.; Chou, L. Y. T.; Vinther, M.; Li, W. A.; Anastassacos, F. M.; Mooney, D. J.; Shih, W. M. Oligolysine-based coating protects DNA nanostructures from low-salt denaturation and nuclease degradation. *Nat. Commun.* **2017**, *8*, 15654.

(55) Kretschy, N.; Sack, M.; Somoza, M. M. Sequence-dependent fluorescence of Cy3- and Cy5-labeled double-stranded DNA. *Bioconjugate Chem.* **2016**, *27* (3), 840−848.

(56) Hilderbrand, S. A.; Weissleder, R. Optimized pH-responsive cyanine fluorochromes for detection of acidic environments. *Chem. Commun.* **2007**, No. 26, 2747−2749.

(57) Khvorova, A.; Watts, J. K. The chemical evolution of oligonucleotide therapies of clinical utility. *Nat. Biotechnol.* **2017**, *35*, 238.

(58) Kosmides, A. K.; Sidhom, J.-W.; Fraser, A.; Bessell, C. A.; Schneck, J. P. Dual targeting nanoparticle stimulates the immune system to inhibit tumor growth. *ACS Nano* **2017**, *11* (6), 5417−5429.

(59) Behlke, M. A. Chemical modification of siRNAs for in vivo use. *Oligonucleotides* **2008**, *18* (4), 305−319.

■ NOTE ADDED AFTER ASAP PUBLICATION

This paper was published ASAP on April 26, 2019, with the Figure 2 graphic in the place of Figure 1. The corrected version was reposted on April 30, 2019.